Direct Optimal Synthesis of a Microwave Bandpass Filter With General Loading Effect

Huan Meng and Ke-Li Wu, *Fellow, IEEE*

***Abstract*—This paper presents a direct approach to the synthesis of a general Chebyshev bandpass filter that matches to a frequency variant complex load. The approach is based on the power wave renormalization theory and two practical assumptions, which are: 1) the prescribed transmission zeros are stationary and 2) the reflection zeros are located along the imaginary axis. Three necessary conditions that stipulate the characteristic polynomials associated to the filter are derived through renormalization of the load reference impedances. It has been shown that these three conditions can only be satisfied by an ideal filter circuit model separated by a piece of interconnecting stub from the complex load. The length of the stub will be optimally designed in the sense that the designed filter will best match to the complex load over a given frequency range. The proposed method offers a deterministic, yet flexible way for optimally designing a diplexer or a multiplexer with a realistic loading effect. The effectiveness of the method is demonstrated by two design examples.**

***Index Terms*—Chebyshev filters, diplexer, filter synthesis, impedance matching, microwave filters.**

I. Introduction

SYNTHESIZING microwave bandpass filters for various specifications is a classic research topic in microwave engineering society over the past half century. A great deal of effort has been devoted to the synthesis of the microwave filters with required characteristics to meet the stringent signal channelization requirements and increasing demands on efficient use of the frequency spectrum for rapid evolution of the wireless communication network. Among many existing synthesis techniques, a direct synthesis technique provides the most optimal and realizable solution.

A direct synthesis approach refers to a deterministic procedure to determine the characteristic polynomials that define a low-pass prototype filter, and then to construct a coupling matrix representation and thereafter to apply similarity transformations for reconfiguration of the filter coupling topology without using any nonlinear optimization techniques. In conventional direct synthesis approaches [1], the terminations at both ports of a filter network are a real constant matched load, which is equivalent to a matched transmission line. Definitely, the loading effect determines the characteristic polynomials of a general Chebyshev filter that has an equiripple reflection characteristic in the passband and a prescribed transmission zero (TZs) arrangement in the rejection bands.

Manuscript received January 02, 2013; accepted May 06, 2013. Date of publication June 04, 2013; date of current version June 28, 2013. This work was supported by the University Grants Committee, Hong Kong Special Administrative Region under Grant AoE/P-04/08.

The authors are with the Department of Electronic Engineering, The Chinese University of Hong Kong, Shatin, Hong Kong (e-mail: klwu@ee.cuhk.edu.hk).

Color versions of one or more of the figures in this paper are available online at http://ieeexplore.ieee.org.

Digital Object Identifier 10.1109/TMTT.2013.2264682

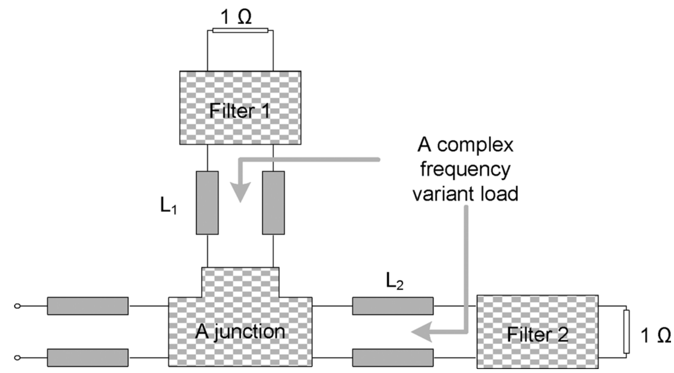

Fig. 1. Channel filters match to complex load.

A loading effect describes the termination condition at one port that is supposed to be matched to an arbitrary load in a given frequency band while the other port is being matched to the unity load. For example, a channel filter in a diplexer has a complex frequency variable loading effect at the port interfaced to the junction while the other port is matched to a unity load, as shown in Fig. 1. The lengths of interconnecting stub [2] between the channel filters and the junction, namely, L_1 and L_2, are very crucial in designing matched channel filters. With inappropriate length, a channel filter could fail to be matched to a complex load. Optimally synthesizing such a channel filter should involve two things, which are: 1) to determine a set of characteristic polynomials that fully describe a coupled resonator filter circuit model and 2) to find a section of transmission line (interconnecting stub) whose characteristic impedance is user defined, with a legitimate length between the filter and the load in the sense that the complex load is optimally matched. Nevertheless, such a practical filter synthesis problem has not been well addressed in the filter design community. Current approaches employed for designing filters matching to a complex load mainly rely on nonlinear optimization [3]. The coupling matrix and the length of the interconnecting stub are simultaneously optimized [4] until a suitable cost function [5], [6] is minimized below the prescribed level. If improper initial values were used, the optimization process would be trapped in a local minimum and could never meet the design requirements. An investigation on optimization constraints of a filter matching to a loading effect was reported in [7].

Research efforts have been continuously devoted to finding the polynomials that define a filter with different loading effects. Early work on direct synthesis with loading effect dates back to 1970s [8], and has been continued by many researchers [9]–[11].

Recently, a direct diplexer synthesis approach was proposed in [12], which is essentially a method of determining the polynomials with the loading effect of a lumped-element Y-junction in shunt connection with the other channel filter. The approach deals with the loading effect that can only be described by a lumped-element circuit model. Three inconveniences of these approaches [8]–[12] are: 1) the complex load is restricted to a limited number of lumped element circuits; 2) high-order polynomials must be dealt with in uncertain accuracy; and 3) no transmission-line effect can be incorporated. An approach was proposed in [13] for handling an arbitrary frequency invariant complex load for narrowband filter design applications. An attempt was made to extend the approach to handle an arbitrary frequency variant complex load by an admittance approach [14]. Two intrinsic limitations to this admittance approach are: 1) it lacks of a mechanism to find a section of interconnecting stub between the load and the filter for optimal impedance matching and 2) there is no rationale in setting up the objective characteristic polynomials, resulting in a network that can never be realized with lumped or distributed elements.

In this paper, a direct optimal synthesis approach to the design of a general Chebyshev bandpass filter that is matched to a general complex loading effect is proposed. The proposed theory is based on the power wave renormalization theory [15] and two practical assumptions, which are: 1) the prescribed TZs are stationary and 2) the reflection zeros are located along the imaginary axis of the complex frequency plane. These two assumptions were also used in [12] where a simple junction circuit model for diplexer design was considered. The first assumption imposes the prescribed filter topology and ensures the rejection-rate satisfy the design requirements; the latter assumption facilitates the synthesis: among various possible transfer functions, synthesis of a Chebyshev filter whose reflection zeros are purely imaginary is an analytical process [1]. Unlike the method presented in [16] by the same authors, where the reflection zeros are determined solely by the prescribed TZs, objective polynomials depend on the complex load, and consequently the reflection zeros are also load dependent in the proposed method. This improvement is very important as the loading effect will be incorporated in setting up a set of realistically objective polynomials with equiripple return-loss characteristic in the passband. In this paper, a general loading effect is defined by the complex impedance over a sufficiently wide band of actual frequency f. The impedance is then transferred to the low-pass domain by the frequency transformation $\omega = f_0/\mathrm{BW}(f/f_0 - f_0/f)$, where BW and f_0 are the bandwidth and center frequency of the filter, respectively. In the discussion below, variable s refers to the complex frequency variable in the low-pass domain. The coupling elements (and matrix) are also defined in the low-pass domain. With the proposed approach, designing a multiplexer or a diplexer becomes a matter of synthesizing an individual channel filter and optimally determining an interconnecting stub for matching to a general complex load.

By introducing a piece of interconnecting stub, designing a matched filter to a generalized complex load with reflection zeros located on imaginary axis can be greatly facilitated. A detailed synthesis procedure is described by a step-by-step procedure. The effectiveness of the method is demonstrated by two design examples.

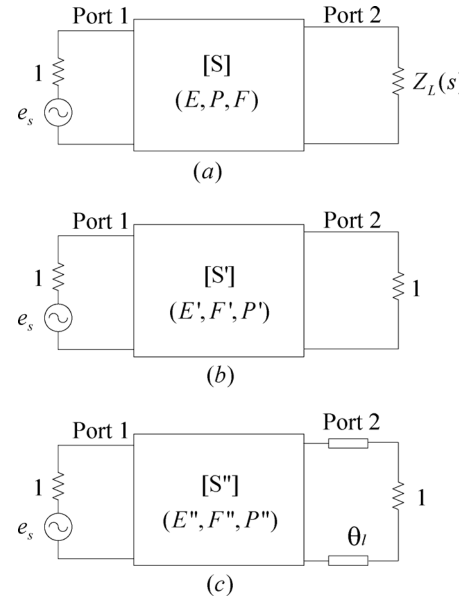

Fig. 2. Same filter network referenced to different reference load and its corresponding approximation.

II. Theory

A. Stipulation Conditions

Considering a matched filter network whose one port is connected to a general frequency variant load and the other port is referenced to the unity load, as shown in Fig. 2(a), to comply with the definition of a coupling matrix, the characteristic polynomials of the filter must be referenced to unity loads at both ports. Directly synthesizing the filter network becomes a matter of finding the characteristic polynomials of the filter that is referenced to the unity load at the two ports and a section of interconnecting stub between the filter and load. The basic concept of the renormalization is illustrated in Fig. 2: the system function [S] in Fig. 2(a) is assumed to be known with port 1 and port 2 connected to the unity load and a general complex load Z_L, respectively. When the reference impedance at port 2 is changed to unity load, the system function $[\mathrm{S}']$ of the same filter network, as defined by Fig. 2(b), can be obtained by power wave renormalization [15] as

$$S'_{22} = \frac{(1 - r_2)(S_{22} - r_2^*)}{(1 - r_2^*)(1 - r_2 S_{22})} \tag{1a}$$

$$S'_{21} = \frac{(1 - r_2)S_{21}}{\sqrt{\mathrm{Re}(Z_L)}(1 - r_2 S_{22})} \tag{1b}$$

where $r_2 = (1 - Z_L)/(1 + Z_L^*)$, * denotes the complex conjugate, and Z_L is the complex impedance at port 2. Although (1) is valid at any frequency band, to comply with the convention in filter synthesis, all the variables are transformed to the low-pass domain in this study. Until now, two sets of characteristic polynomials have been defined: one describes the objective filter responses defined by [S] with

$$S_{22} = \frac{F(s)}{E(s)} \quad S_{21} = \frac{P(s)}{\varepsilon E(s)} \tag{2a}$$

and the other specifies the measurable response of [S′] of the same filter network, which is referenced to the unity load

$$S'_{22} = \frac{F'(s)}{E'(s)} \quad S'_{21} = \frac{P'(s)}{\varepsilon' E'(s)}. \tag{2b}$$

Although the characteristic polynomials are defined in the complex plane, in evaluating (1) and (2), s will be stipulated to $s = j\omega$ as only ω is measurable frequency. Defining characteristic polynomials in the complex plane is to find wide sense defined system functions that best satisfy various filter performance requirements along the $s = j\omega$ axis. Substituting (2) into (1) and using the equation of the conservation of power, the polynomials defining [S′] can be obtained by

$$P'(s) = 2\sqrt{\mathrm{Re}(Z_L(s))}P(s)/\varepsilon \quad \text{(Transference)} \tag{3a}$$
$$F'(s) = (1 + Z_L(s))F(s) - (1 - Z_L^*(s))E(s) \quad \text{(Matchability)} \tag{3b}$$
$$E'(s) = (1 + Z_L^*(s))E(s) - (1 - Z_L(s))F(s) \quad \text{(Conservativeness).} \tag{3c}$$

The equations in (3) are the conditions stipulating the objective polynomials $F(s)$, $E(s)$, and $P(s)$ and the polynomials $F'(s), E'(s)$, and $P'(s)$ that describe an approximation of the corresponding measurable responses. Again, the validation domain for s when evaluating (3) is alone the $j\omega$ axis. For a general loading effect in a broadband sense, it is impossible to find a set of solutions that satisfy (3) in the entire frequency band. However, one can find a set of optimally approximated and realizable solutions of $E'(s)$ and $F'(s)$ by conveniently choosing the same order of $E(s)$ and $F(s)$, respectively, to satisfy (3) over a given frequency band. The choice allows the order and the coupling topology of the filter to be fixed.

It will be approved later in this paper that a good approximate solution to (3) can be achieved by a realizable filter network [S″] and a section of interconnecting stub between the load and the filter network. It will be shown that the filter network [S″] is measurable as it is referenced to the unity load at both ports, as shown in Fig. 2(c), and most importantly it can be described by a coupled resonator bandpass filter circuit model. In the proposed approach, an optimal length of the interconnecting stub will be determined in the sense that the conservativeness condition in (3) is optimally satisfied under the two proposed assumptions.

B. Direct Synthesis Approach

It is apparent from (3) that the characteristic polynomials of the filter network to be designed depend on the loading effect Z_L as well as the objective polynomials $F(s)$,$E(s)$, and $P(s)$. Therefore, the objective polynomials must be achievable, load dependent, and satisfy the required specifications. The proposed synthesizing approach starts with finding a set of legitimate objective polynomials. The detailed step-by-step procedure is given by the following steps.

Step 1) Stipulating the measurable polynomial $P'(s)$ as

$$P'(s) = \frac{1}{\varepsilon'} e \prod_{i}^{nfz} (s - p'_i) \tag{4}$$

where p'_i refers to the ith prescribed TZ and nfz denotes the number of TZs. In addition, ε' and θ_p are two unknown parameters to be determined and can be temporally set to 1 and 0, respectively. In practice, a proper selection of prescribed TZs would ensure the required rejections and group delay for a filter of a given order. Note that the TZs need to be symmetric about the imaginary axis.

Step 2) Determining the objective polynomial $P(s)$ by the transference condition (3a) using linear least squares fitting [17] over the passband of the designed filter. To avoid an ill-posed problem, the number of samples should be at least larger than the filter order N plus one. In general, 50 or more points are suggested. The order of $P(s)$ can be increased to fully reflect the effect of frequency variant load and to minimize the least square error. Denote the roots of $P(s)$ as p_i, $i = 1, 2, \ldots, k$, where k is smaller than N. It is apparent that, according to the transference condition, $P(s)$ not only shares the TZs of $P'(s)$, but also possibly incorporates extra zeros caused by the complex load. It will be shown later that the synthesized filter network will possess the same TZs as those of $P'(s)$. This is called TZ stationary property.

Step 3) Synthesizing the objective polynomials $F(s)$ and $E(s)$ and the normalization constant ε that satisfy a general Chebyshev characteristic with p_i, $i = 1, 2, \ldots, k$, obtained in Step 2, the prescribed return-loss level *RL* in decibels and the filter order N. To this end, a well-established procedure is available in [1]. In this step, the normalization constant ε' will be updated by $\varepsilon' = \varepsilon$.

Step 4) With a set of realistic objective polynomials $P(s), F(s)$, and $E(s)$ known, $F'(s)$ can be approximately obtained using matchability condition (3b) by linear least square fitting with the same order as that of $F(s)$. It must be noted that $F'(s)$ is not *monic* and its coefficient of the Nth-order term is a complex number in general and can be expressed as $f'_N = |f'_N|e^{j\theta_f}$.

Step 5) Having had known $P'(s)$ (in Step 1), ε' and $F'(s)$ (in Step 3 and Step 4, respectively), the roots s_i [the ith zero of the polynomial $E'(s)$] and $|e'_N|$ of the objective polynomial $E'(s)$ can be determined using the conservation of power equation

$$E'(s)E'(s)^* = F'(s)F'(s)^* + P'(s)P'(s)^*/\varepsilon'^2 \tag{5}$$

where e'_N is the coefficient of the Nth-order term of $E'(s)$ and $|\cdot|$ refers to the magnitude. It is apparent that $|e'_N| = |f'_N|$, whereas the phase of e'_N, θ_e, can be optimally selected to minimize the error in satisfying conservativeness condition (3c) defined by

$$\text{error} = \sqrt{\frac{1}{M}\sum_{i=1}^{M} |E'(j\omega_i) - f(j\omega_i)|^2} \tag{6}$$

where $f(j\omega_i)$ denotes the numerical value of the right-hand side of (3c) at the ith sampling frequency in the low-pass domain. Note that although the system $P'(s), F'(s)$, and $E'(s)$ is measurable, it does not necessarily describe a coupled resonator filter circuit model because, in general, $\theta_e \neq \theta_f$.

Step 6) Specifying a set of new polynomials $E''(s), P''(s)$, and $F''(s)$ from the system $P'(s), F'(s)$, and $E'(s)$ by

$$F'(s) = \sum_{i=0}^{N} f_i' s^i = f_N' \sum_{i=0}^{N} (f_i'/f_N') s^i = |f_N'| e^{j\theta_f} F''(s) \tag{7a}$$

$$E'(s) \approx |f_N'| e^{j\theta_e} \prod_{i=1}^{N} (s - s_i) = |f_N'| e^{j\theta_e} E''(s) \tag{7b}$$

$$P'(s) = e^{j\theta_p} P''(s) \tag{7c}$$

where f_i' is the coefficient of the ith-order term of $F'(s)$. The approximation sign in (7b) means that (3c) can be optimally satisfied by adjusting phase θ_e. By normalizing to the highest coefficients e_N' and f_N', respectively, the resultant $E''(s), P''(s)$, and $F''(s)$ can fully describe a coupled resonator filter network because they satisfy the following conditions:

1) power conservation;
2) roots of $E''(s)$ reside in the left half of complex plane;
3) roots of $P''(s)$ are symmetric about the imaginary axis;
4) polynomials $E''(s)$, $P''(s)$, and $F''(s)$ are *monic*.

According to (2b), the scattering parameters of a measurable network that is matched to a general complex load in a given frequency band can thus be expressed as

$$S_{22}' = \frac{F'(s)}{E'(s)} = \frac{|f_N'| e^{j\theta_f} F''(s)}{|f_N'| e^{j\theta_e} E''(s)} = e^{-j2\theta_l} \frac{F''(s)}{E''(s)} \tag{8a}$$

$$S_{21}' = \frac{P'(s)}{\varepsilon' E'(s)} = \frac{e^{j\theta_p} P''(s)}{\varepsilon' |f_N'| e^{j\theta_e} E''(s)} = e^{-j\theta_l} \frac{P''(s)}{\varepsilon'' E''(s)} \tag{8b}$$

where the relations $\theta_l = (\theta_e - \theta_f)/2, \theta_p = (\theta_e + \theta_f)/2$, and $\varepsilon'' = \varepsilon' \cdot |f_N'|$ are implied. Equation (8) reveals that the network, which best matches to the general complex loading in a given frequency band, consists of an ideal coupled resonator filter defined by polynomials $F''(s)$, $E''(s)$, and $P''(s)$ and a section of optimally designed interconnecting stub θ_l between the ideal filter and load. The electrical length is optimal in the sense that it minimizes the error in satisfying conservativeness condition (3c). This mixed network is depicted in Fig. 2(c). It is a common practice that the characteristic impedance of the interconnecting stub is user defined and is used in measuring the value of the complex load. Although the phase constant θ_l is frequency independent, it represents a very good approximation of a piece of transmission by the electric length at the center frequency of a passband filter and is irrelevant to the dispersive relation of a particular type of transmission line. For most of the channel filter applications, where the fractional bandwidth is only about a few percent, this approximation works very well.

It is seen that θ_p is found at the last stage and theoretically $P'(s)$ should be updated accordingly. However, θ_p takes no effect in the proposed procedure since it only contributes a constant phase to $P'(s)$ and consequently $P(s)$, whereas the roots p_i will not be altered. The phase provision θ_p is introduced in (4) in order to ensure $P''(s)$ be realizable as $P''(s) = e^{-j\theta_p} P'(s)$.

Under the assumption that the reflection zeros are located along the imaginary axis, the combined filter and an ideal transmission line network does not always ensure a perfect impedance matching. Such mismatching is reflected by the minimal error in searching for an optimal θ_e by applying conservativeness condition 3(c). It is found that the matching condition can be improved when the complex load presents more stationary variation versus frequency.

III. Practical Design Examples

A. Diplexer Design Using an H-Plane T-Junction

To illustrate the effectiveness of the proposed method, the detailed design procedure for an H-plane waveguide diplexer is given here. The diplexer has two fourth-order all-pole filters connected to a WR62 H-plane T-junction. An iterative approach is applied to each channel filter design until the diplexer error, which is defined as

$$\text{diplexer error} = \sqrt{\sum_{i}^{2} (\text{minimum error of } i\text{-th channel})^2} \tag{9}$$

is below a certain threshold value, where the error of the ith channel is given by (6). Equivalently, the complex load faced by each filter is iteratively adjusted until the matching error of each filter is small enough by adjusting the length of the interconnecting stub. The center frequencies of the two channel filters in this example are 15 and 15.25 GHz, respectively, the targeted return loss is 22 dB, and the bandwidth is 0.2 GHz for both filters. The initial lengths of the stubs connected to the low channel and high channel are $L_L = 16.5$ mm and $L_H = 10.5$ mm, respectively. The frequency response of the waveguide T-junction is obtained through a full-wave mode-matching electromagnetic (EM) software. Initially, the coupling matrices for both filters are generated by a conventional direct synthesis method with a real constant terminal impedance.

Fig. 3 shows the complex load faced by the high channel filter in the second iteration, normalized to the characteristic impedance of a WR62 waveguide. Following the procedure given in Section II, the characteristic polynomials $E''(s), P''(s)$, and $F''(s)$ together with θ_l of the high channel filter after the second iteration are given in Table I(a). For comparison, the synthesis approach [13] is repeated here with the constant complex load of $Z_L = 0.5434 + 0.4737i$ at $f = 15.25$ GHz.

The obtained polynomials are reported in Table I(b). It can be foreseen that when the complex load is a constant, only the I/O coupling and the self-coupling that are immediately next to the load get affected from that with the real load. Fig. 4 compares the synthesized diplexer responses using the proposed approach (including the dispersion effect) and the approach in [13] after

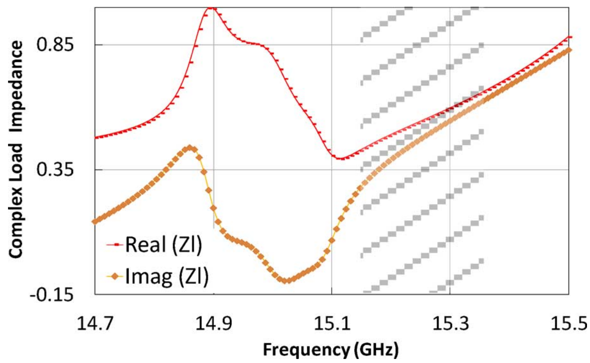

Fig. 3. Normalized complex load faced by high channel filter in second iteration.

TABLE I
COUPLING MATRICES FOR HIGH CHANNEL FILTER AFTER SECOND ITERATION, (a) USING PROPOSED APPROACH, (b) USING APPROACH [13]

0	1.101	0	0	0	0
1.101	-0.004	0.982	0	0	0
0	0.982	-0.019	0.753	0	0
0	0	0.753	-0.206	1.294	0
0	0	0	1.294	-2.275	1.524
0	0	0	0	1.524	0

(a)

0	1.082	0	0	0	0
1.082	0	0.960	0	0	0
0	0.960	0	0.727	0	0
0	0	0.727	0	0.960	0
0	0	0	0.960	-1.021	1.468
0	0	0	0	1.468	0

(b)

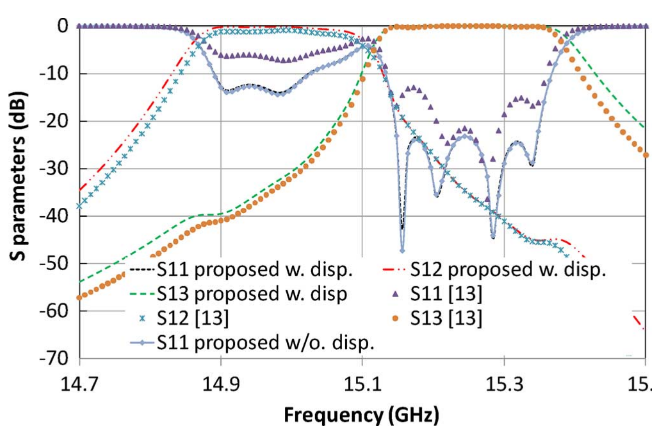

Fig. 4. Comparison of proposed approach and the approach in [13].

the second iteration of the high channel filter. To account for the dispersion effect, the electrical length θ_l is converted to the absolute length of the stub by $l = \lambda_{g0}\theta_l/(2\pi)$, where λ_{g0} is the guided wavelength at the center frequency. It is clear that the proposed method outperforms the approach in [13] because frequency variation of the loading effect is taken into consideration. In addition, the common port return loss with a constant phase θ_l is also shown in Fig. 4 for comparative purposes. It is apparent that the difference between the return loss with a dispersion effect and that without a dispersion effect is very insignificant. Similar negligible deviations are observed for S_{21} and S_{31}, but are not shown in Fig. 4 for clarity.

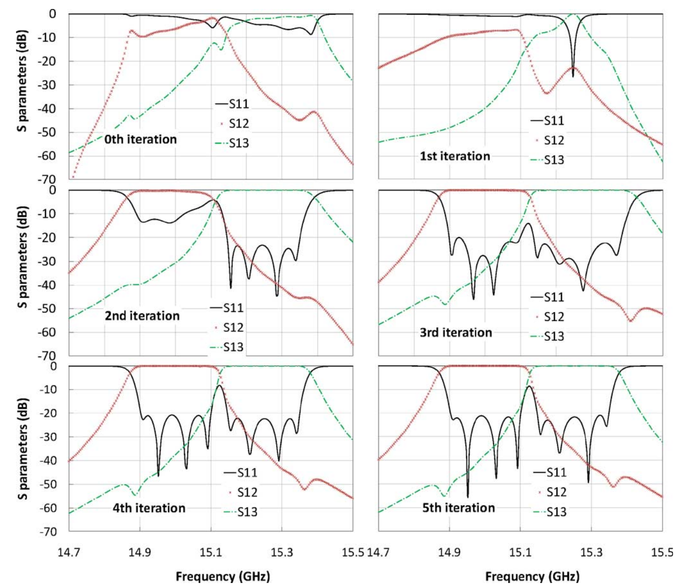

Fig. 5. Responses for each iteration of the waveguide diplexer design.

The same procedure is applied to the low channel filter alternatively until convergence is achieved. Fig. 5 shows the circuit model response in the diplexer design at each iteration while the obtained normalized coupling matrices are summarized in Table II(a) and the characteristic polynomials $E''(s), P''(s)$, and $F''(s)$ for both channels after the fourth iteration are summarized in Table II(b). The normalized coupling matrix can be easily converted to a de-normalized matrix with the prescribed center frequency and bandwidth of each filter. It can be observed that the difference in the coupling values between the fourth iteration and fifth iteration is insignificant, and thus it can be judged that the synthesis approaches to a satisfactory convergence only by four iterations despite of a poor initial value. It is also worth noting that the reflection zeros are not always along the imaginary axis although they are imposed to be. The shift of reflection zeros in the complex plane is due to the mixed transmission line plus filter network being only an approximated optimal solution. Unless the error in (6) becomes zero, in general there is always a tiny mismatch, and hence, a possible shift of reflection zeros when the filter is connected to the complex load. However, when the error is close to zero, for example, in the order of 10^{-3}, this shift contributes little to the return-loss level.

Fig. 6 shows the error defined in (6) with a different length of connecting stub in the fourth iteration for the high channel filter when applying condition 3(c). It can be seen that the length of the stub is very crucial in minimizing the error.

Fig. 7 shows the minimum error for each channel filter, together with the diplexer error after each iteration. It is seen that diplexer error approaches zero monotonically as the number of iteration increases, whereas the minimum error of each individual channel filter may have some fluctuations. Therefore, the diplexer phase error is used as an indicator for convergence.

Having had the coupling matrices synthesized, the physical dimensions of the channel filters can be obtained based on [2]. Fig. 8 shows the dimensions of the EM model based on the synthesized coupling matrices; an extra $\lambda/4$ transmission line is inserted between each channel filter and the junction to invert the

TABLE II
(a) COUPLING MATRICES, INTERCONNECTING STUB LENGTH AND MATCHING ERRORS FOR EACH ITERATION OF THE WAVEGUIDE DIPLEXER DESIGN EXAMPLE, (b) THE FINAL CHARACTERISTIC POLYNOMIALS AFTER FOURTH ITERATION

(a)

Low Channel						
	0th	1st	2nd	3rd	4th	5th
M_{01}	1.082	1.949	1.500	1.14	1.043	1.048
M_{12}	0.960	2.439	1.445	1.009	0.905	0.911
M_{23}	0.727	1.084	0.783	0.713	0.676	0.680
M_{34}	0.960	0.697	0.657	0.760	0.755	0.764
M_{45}	1.082	0.294	0.559	0.622	0.606	0.607
M_{11}	0.000	1.817	0.484	-0.114	-0.027	-0.022
M_{22}	0.000	0.983	0.253	-0.058	-0.009	-0.007
M_{33}	0.000	0.361	0.214	0.025	0.033	0.032
M_{44}	0.000	-0.447	0.138	-0.035	0.019	0.022
l_L^0(mm)	16.5	21.771	16.986	17.923	18.11	18.252
error		0.2642	0.3319	0.0356	0.0219	0.0191
High Channel						
	0th	1st	2nd	3rd	4th	5th
M_{01}	1.082	1.120	1.101	1.168	1.047	1.040
M_{12}	0.960	0.987	0.982	1.099	0.911	0.903
M_{23}	0.727	0.738	0.753	0.829	0.681	0.675
M_{34}	0.960	0.368	1.294	0.908	0.752	0.744
M_{45}	1.082	1.004	1.524	0.688	0.600	0.593
M_{11}	0.000	0.025	-0.004	-0.153	0.002	0.018
M_{22}	0.000	0.040	-0.019	-0.195	-0.005	0.004
M_{33}	0.000	0.072	-0.206	-0.266	-0.038	-0.003
M_{44}	0.000	1.708	-2.275	-0.346	-0.058	-0.029
l_H^0(mm)	10.5	13.656	15.082	16.446	16.477	16.383
error		0.417	0.0168	0.032	0.0203	0.0213

(b)

Low Channel			
$E''(s)$	$s^4+(1.4556 + 0.0159i)\ s^3+(2.2467 + 0.0449i)\ s^2+(1.5867 + 0.0278i)\ s+(0.6940 + 0.0088i)$		
$P''(s)$	1.00 i		
$F''(s)$	$s^4+(0.7197+0.0159i)\ s^3+(1.4464+0.0466i)\ s^2+(0.6470+0.0087i)\ s+(0.2827-0.0026i)$		
θ_l	0.3802 rad	ε''	1.7114
High Channel			
$E''(s)$	$s^4+(1.4569 - 0.0994i)\ s^3+(2.2517 - 0.1259i)\ s^2+(1.5918 - 0.1248i)\ s+(0.6507 - 0.0436i)$		
$P''(s)$	1.00 i		
$F''(s)$	$s^4+(0.7383-0.0994i)\ s^3+(1.4629-0.0959i)\ s^2+(0.6617-0.0906i)\ s-(0.2581-0.0211i)$		
θ_l	1.4845 rad	ε''	1.7059

phase of the physical filter since the phase of S_{11} for a waveguide filter at high frequency approaches to 180°, whereas that defined by characteristic polynomials approaches to 0°. In the physical EM model, the thickness for all irises is 0.5 mm. The S-parameters from the synthesized filter circuit model and those from the EM designed model are compared in Fig. 9. The result of the circuit model with a $\lambda/4$ long waveguide at the center frequency inserted is identical to that of the EM designed model,

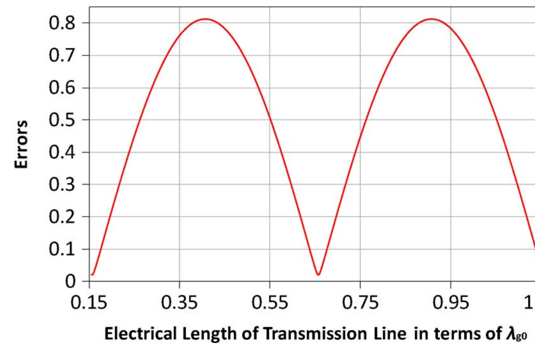

Fig. 6. Error versus interconnecting stub length at fourth iteration of high channel.

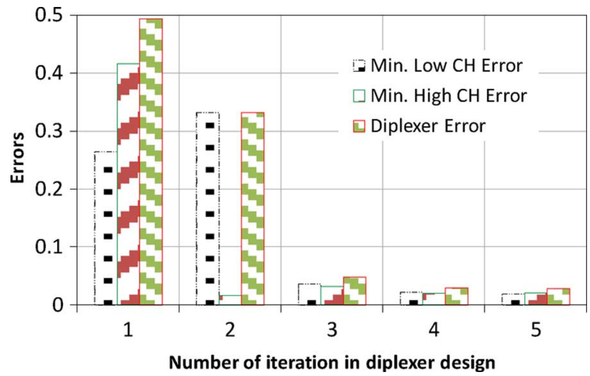

Fig. 7. Errors versus number of iterations in diplexer design.

Low channel		High channel	
l	w	l	w
l_L^0=24.568	w_L^{01}=4.716	l_H^0=22.761	w_H^{01}=4.612
l_L^1=12.153	w_L^{12}=2.760	l_H^1=11.834	w_H^{12}=2.685
l_L^2=12.579	w_L^{23}=2.645	l_H^2=12.239	w_H^{23}=2.583
l_L^3=12.547	w_L^{34}=2.954	l_H^3=12.216	w_H^{34}=2.888
l_L^4=11.765	w_L^{45}=5.701	l_H^4=11.466	w_H^{45}=5.603
a= 15.8			

Units: mm

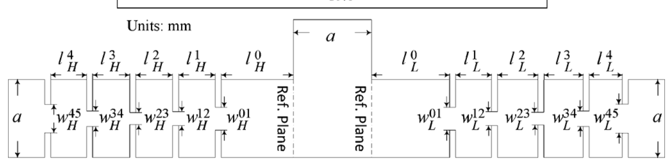

Fig. 8. Physical model of the designed H-plane waveguide diplexer.

and therefore is not presented. The deviation between the results of the synthesized filter circuit model and that of the EM model is introduced by the dispersive $\lambda/4$ long waveguide. It is seen that the proposed approach is more specified to filters with shunt LC resonators, whose reflection coefficient has a zero phase at $\omega = \infty$. For the filters with series LC resonators, on the other hand, adding an extra $\lambda/4$ transmission line will introduce a tolerable error.

It should be mentioned that the proposed method is only limited to noncontiguous cases in which the common port return loss in the passband of each channel filter can be well approximated by the polynomials. When two channels are very close, e.g., less than 1% bandwidth, this assumption will be violated. Nevertheless, the solution by this method can still serve as a good initial point for further optimization.

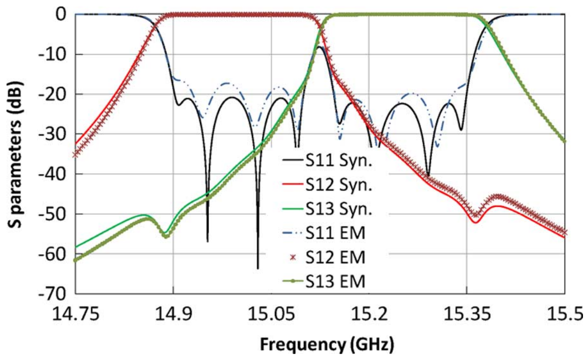

Fig. 9. S-parameters of synthesized circuit model and EM designed model of an H-plane waveguide diplexer.

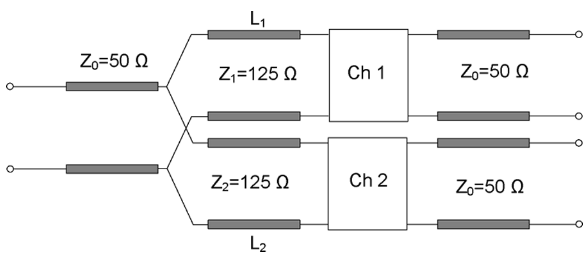

Fig. 10. Circuit schematic of a coaxial resonator diplexer with a transmission line Y-junction.

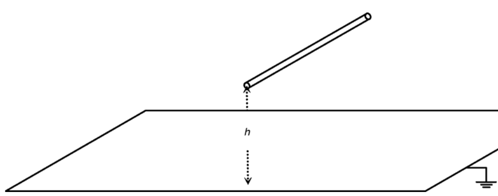

Fig. 11. Grounded wire line for realizing the transmission line between the Y-junction and the coaxial resonator channel filters.

B. Coaxial Resonator Diplexer With a Wired Y-Junction

The design process of a coaxial combline diplexer consisting of a GSM channel and a CDMA channel is described in this example. The channel filters are connected to the common port through a grounded wire line Y-junction whose characteristic impedances are $Z_0 = 50\Omega, Z_1 = Z_2 = 125\ \Omega$, as illustrated in Fig. 10. The characteristic impedance Z_1 and Z_2 are defined by the grounded wire transmission line, as shown in Fig. 11, where $h = 2.25$ mm and the radius of conducting wire is 0.75 mm. The channel filters are initially designed as seventh order and 25-dB return loss by the conventional direct synthesis method with the assumption that the terminated impedance is a real constant value. The center frequencies of channels 1 and 2 are 850 and 940 MHz, respectively, and the bandwidths of both filters are 55 MHz. A TZ at 910 MHz is prescribed for channel 1 and the other TZ is prescribed at 890 MHz for channel 2. Initially L_1 and L_2 are arbitrarily selected to be $L_1 = 19$ mm and $L_2 = 22$ mm.

Starting from the low channel filter, two channel filters are synthesized alternatively by the proposed approach. The solution converges after two iterations. Since the characteristic impedance at each port of the filter is different, those polynomials should be further renormalized to 125 Ω. Table III shows the coupling matrices obtained for both channels after re-normalization. The final interconnecting stub lengths are $L_1 =$ 10.6 mm and $L_2 = 20.6$ mm. For validation purposes, the designed diplexer has been fabricated. The required positive and negative cross-couplings are realized with capacitive and inductive probes, respectively. A photograph of the fabricated diplexer is shown in Fig. 12. It can be seen that two designed sections of interconnecting stubs are realized using two pieces of wires extended from the Y-junction with the housing wall as the natural ground. Since the resonators are shunt LC type, there is no need to add an extra $\lambda/4$ transmission line. The Q factor for both channel filters is about 2200. Finally, the measurement responses together with those from the synthesized diplexer circuit model are superimposed in Fig. 13. Good agreement demonstrates that the proposed approach can provide a true realistic filter circuit model in practical applications.

TABLE III
COUPLING MATRICES FOR THE COAXIAL DIPLEXER

Low Channel				High Channel			
m_{01}	1.826	m_{11}	0.005	m_{01}	1.821	m_{11}	-0.011
m_{12}	0.987	m_{22}	0.010	m_{12}	0.983	m_{22}	-0.013
m_{23}	0.655	m_{33}	0.015	m_{23}	0.652	m_{33}	-0.020
m_{34}	0.572	m_{44}	-0.339	m_{34}	0.551	m_{44}	0.428
m_{45}	0.573	m_{55}	0.013	m_{45}	0.551	m_{55}	-0.020
m_{56}	0.646	m_{66}	0.067	m_{56}	0.650	m_{66}	-0.030
m_{67}	0.920	m_{77}	0.015	m_{67}	0.920	m_{77}	-1.279
m_{78}	1.946	m_{35}	0.184	m_{78}	1.569	m_{35}	-0.235

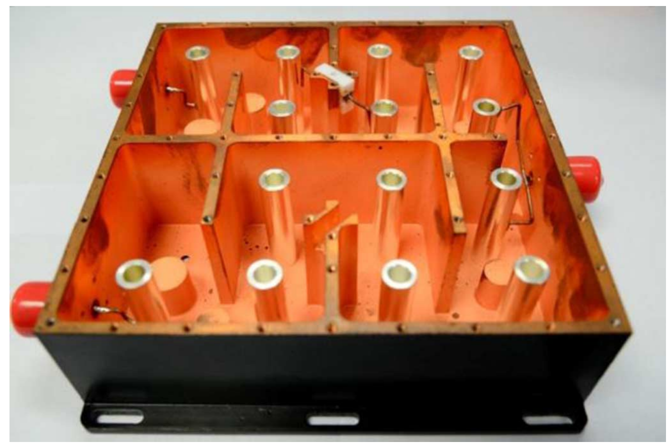

Fig. 12. Photograph of the fabricated diplexer with top lid removed.

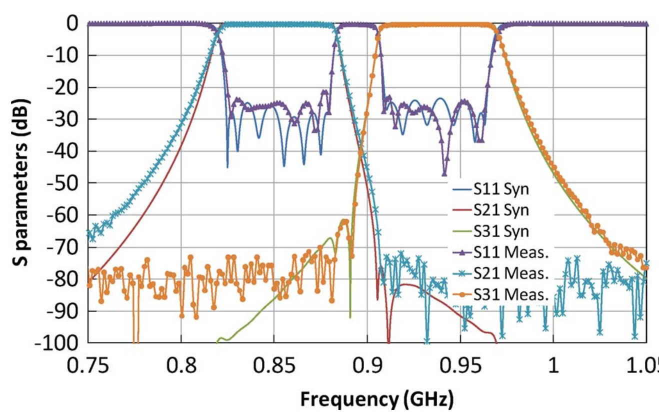

Fig. 13. S-parameters of the synthesized and the measured responses of a coaxial resonator diplexer.

IV. Conclusion

A direct optimal synthesis method for a microwave bandpass filter with a general loading effect is proposed in this paper. Two legitimate assumptions are imposed: the prescribed TZs are stationary when the load changes and the reflection zeros are distributed along the imaginary axis of a complex frequency plane. By using the power wave renormalization, a set of conditions are developed and used for determining a set of realistic and load dependent objective polynomials, with which a new set of polynomials that describe the measurable filter responses of the targeted filter can be derived in accordance. It has been approved that this set of new polynomials can be very well approximated by an ideal filter circuit model cascaded by a piece of transmission line. The length of the transmission line is designed in an optimal sense that the matching conditions are satisfied in a best effort. The detailed design procedure is provided. The effectiveness of the proposed method has been demonstrated through two practical design examples. It has been shown that the proposed approach provides a robust and flexible design tool for the design of a bandpass filter with a complex load.

References

[1] R. J. Cameron, "General coupling matrix synthesis methods for chebyshev filtering functions," *IEEE Trans. Microw. Theory Techn.*, vol. 47, no. 4, pp. 433–422, Apr. 1999.

[2] R. J. Cameron, C. M. Kudsia, and R. R. Mansour, *Microwave Filters for Communication Systems: Fundamentals, Design and Application*. Hoboken, NJ, USA: Wiley, 2007, ch. 13, p. 494.

[3] M. Yu and Y. Wang, "Synthesis and beyond," *IEEE Microw. Mag.*, vol. 12, no. 6, pp. 62–76, Oct. 2011.

[4] R. J. Cameron and M. Yu, "Design of manifold-coupled multiplexers," *IEEE Microw. Mag.*, vol. 8, no. 5, pp. 46–59, Oct. 2007.

[5] M. Guglielmi, "Optimum CAD procedure for manifold diplexers," in *IEEE MTT-S Int. Microw. Symp. Dig.*, 1993, pp. 1081–1084.

[6] Y. Rong, H.-W. Yao, K. A. Zaki, and T. G. Dolan, "Millimeter-wave Ka-band H-plane diplexers and multiplexers," *IEEE Trans. Microw. Theory Techn.*, vol. 47, no. 12, pp. 2325–2330, Dec. 1999.

[7] A. Morini and T. Rozzi, "Constrains to the optimum performance and bandwidth limitations of diplexers employing symmetric three-port junctions," *IEEE Trans. Microw. Theory Techn.*, vol. 44, no. 2, pp. 242–248, Feb. 1996.

[8] J. L. Haine and J. D. Rhodes, "Direct design formulas for asymmetric bandpass channel diplexer," *IEEE Trans. Microw. Theory Techn.*, vol. MTT-25, no. 10, pp. 807–814, Oct. 1977.

[9] J. D. Rhodes and R. Levy, "A generalized multiplexer theory," *IEEE Trans. Microw. Theory Techn.*, vol. MTT-27, no. 2, pp. 99–111, Feb. 1979.

[10] J. D. Rhodes and R. Levy, "Design of general manifold multiplexer," *IEEE Trans. Microw. Theory Techn.*, vol. MTT-27, no. 2, pp. 111–123, Feb. 1979.

[11] R. Levy, "Synthesis of non-contiguous diplexers using broadband matching theory," in *IEEE MTT-S Int. Microw. Symp. Dig.*, Boston, MA, USA, Jun. 10–14, 1991, pp. 543–546.

[12] G. Macchiarella and S. Tamiazzo, "Novel approach to the synthesis of microwave diplexers," *IEEE Trans. Microw. Theory Techn.*, vol. 54, no. 12, pp. 4281–4290, Dec. 2006.

[13] K.-L. Wu and W. Meng, "A direct synthesis approach for microwave filters with a complex load and its application to direct diplexer design," *IEEE Trans. Microw. Theory Techn.*, vol. 55, no. 5, pp. 1010–1017, May 2007.

[14] M. Meng and K.-L. Wu, "Direct synthesis of general Chebyshev bandpass filters with a frequency variant complex load," in *IEEE MTT-S Int. Microw. Symp. Dig.*, Anaheim, CA, USA, May 2010.

[15] K. Kurokawa, "Power waves and the scattering matrix," *IEEE Trans. Microw. Theory Techn.*, vol. MTT-13, no. 3, pp. 194–202, Mar. 1965.

[16] H. Meng and K.-L. Wu, "Direct optimal synthesis of microwave bandpass filters with a general loading effect," in *IEEE MTT-S Int. Microw. Symp. Dig.*, Montreal, QC, Canada, Jun. 2012.

[17] E. Kreyszig, *Advanced Engineering Mathematics*. New York, NY, USA: Wiley, 2005, ch. 20, pp. 860–862.

Huan Meng received the B.Eng. degree (with first-class honors) in electronic and information engineering from The Hong Kong Polytechnic University, Hung Hom, Hong Kong, in 2010, and the M.Phil. degree in electronic engineering from The Chinese University of Hong Kong, Shatin, Hong Kong, in 2012.

Since 2012, he has been a Research Assistant with the Department of Electronic Engineering, The Chinese University of Hong Kong. His research is mainly focused on the design and synthesis of passive microwave components, particularly microwave diplexers.

Mr. Meng was the recipient of the Asia–Pacific Microwave Conference Prize in 2012.

Ke-Li Wu (M'90–SM'96–F'11) received the B.S. and M.Eng. degrees from the Nanjing University of Science and Technology, Nanjing, China, in 1982 and 1985, respectively, and the Ph.D. degree from Laval University, Quebec, QC, Canada, in 1989.

From 1989 to 1993, he was with the Communications Research Laboratory, McMaster University, as a Research Engineer and a Group Manager. In March 1993, he joined the Corporate Research and Development Division, COM DEV International (the largest Canadian space equipment manufacturer), where he was a Principal Member of Technical Staff. Since October 1999, he has been with The Chinese University of Hong Kong, Shatin, Hong Kong, where he is currently a Professor and the Director of the Radiofrequency Radiation Research Laboratory (R3L). He has authored or coauthored numerous publications in the areas of electromagnetic (EM) modeling and microwave passive components, microwave filters, and antenna engineering. His current research interests include partial element equivalent circuit (PEEC) and derived physically expressive circuit (DPEC) EM modeling of high-speed circuits, RF and microwave passive circuits and systems, synthesis theory and practices of microwave filters, antennas for wireless terminals, low-temperature co-fired ceramic (LTCC)-based multichip modules (MCMs), and RF identification (RFID) technologies. His research group is the main workforce in various active RFID research and applications in Hong Kong.

Prof. Wu is a member of the IEEE MTT-8 Subcommittee (Filters and Passive Components). He serves as a Technical Program Committee (TPC) member for many prestigious international conferences including the IEEE Microwave Theory and Techniques Society (IEEE MTT-S) International Microwave Symposium (IMS). He was an associate editor for the IEEE Transactions on Microwave Theory and Techniques (2006–2009). He was the recipient of the 1998 COM DEV Achievement Award for the development of exact EM design software of microwave filters and multiplexers and the Asia–Pacific Microwave Conference Prize in 2008 and 2012.